

The topology of the molecular charge distribution and the electric field gradient at the N atom in nitriles

Yosslen Aray and Juan Murgich

Citation: *The Journal of Chemical Physics* **91**, 293 (1989); doi: 10.1063/1.457515

View online: <http://dx.doi.org/10.1063/1.457515>

View Table of Contents: <http://scitation.aip.org/content/aip/journal/jcp/91/1?ver=pdfcov>

Published by the AIP Publishing

Articles you may be interested in

[The electric field gradient at the N nuclei and the topology of the charge distribution in the protonation of urea](#)
J. Chem. Phys. **101**, 9800 (1994); 10.1063/1.467945

[The topology of the charge distribution and the electricfield gradient at the N nucleus in imines and diimides](#)
J. Chem. Phys. **97**, 9154 (1992); 10.1063/1.463341

[Quantum topology of molecular charge distributions. III. The mechanics of an atom in a molecule](#)
J. Chem. Phys. **73**, 2871 (1980); 10.1063/1.440457

[Quantum topology of molecular charge distributions. II. Molecular structure and its change](#)
J. Chem. Phys. **70**, 4316 (1979); 10.1063/1.438006

[Charge Distribution and Electric Field Gradients in Ionic Crystals](#)
J. Chem. Phys. **35**, 1032 (1961); 10.1063/1.1701107



The topology of the molecular charge distribution and the electric field gradient at the N atom in nitriles

Yosslen Aray^{a)} and Juan Murgich^{b)}

Centro de Química, Instituto Venezolano de Investigaciones Científicas, (IVIC), Apartado 21827, Caracas 1020A, Venezuela

(Received 27 December 1988; accepted 1 March 1989)

A direct relationship between the N valence shell charge topology reflected in its Laplacian and the components of the electric field gradient (EFG) at the N nucleus in nitriles was found. The largest diagonal component of the N EFG tensor was showed to be determined by the combined effect of the bonded and nonbonded maxima of the Laplacian of the valence shell of the N atom along the C–N direction. In nonlinear nitriles, the asymmetry of the N field gradient around the C–N direction was showed to be determined by the difference in the values of the maxima of the Laplacian of the valence shell obtained in two mutually perpendicular planes that are also normal to the C–N direction and contained the N nucleus.

INTRODUCTION

The chemical properties of a molecule are determined by the morphology of the electronic charge distribution and by its evolution in time. Several experimental methods have been used to obtain information about that charge distribution.^{1,2} In particular, the interaction between the nuclear electric quadrupole moment and the external electric field gradient (EFG) has been extensively used for that purpose.² The EFG tensor is very sensitive to changes introduced in the charge distribution so that information about the effects of substitution, charge transfer, hydrogen bonds, and complex formation, may be obtained from the study of the EFG present at sites containing a quadrupolar nucleus.² The interpretation of the changes observed in the EFG have been made in terms of the population of certain molecular orbitals or localized molecular orbitals.² Consequently, lone pairs, σ and π orbitals connected with the Lewis theory of electron pairs¹ have been extensively used in the interpretation of the EFG and of its changes.² Nevertheless, it is known that the possibility of representing the charge distribution in terms of localized orbitals does not imply the existence of localized electron pairs.³ Experimental and theoretical results^{3–5} show that no localized pair of electrons are present in the total molecular electronic density $\rho(\mathbf{r})$. Clearly, a new way of defining atoms and their interactions based in observables like ρ rather than in a more or less arbitrary sets of orbitals is then necessary. Such an approach was developed by Bader and co-workers^{3–5} in terms of the topology of the total electronic density. Unambiguous definitions derived from fundamental topological properties of the total charge density for both atoms in molecules and chemical bonds have been obtained.^{3–5} It has been found that the structure and stability of a molecular system is determined by the gradient vector field $\nabla\rho$. On the other hand, it has been shown that the Laplacian of $\rho(\mathbf{r})$ identifies regions of space wherein the charge density is either locally concentrated or depleted.⁶ The Laplacian of

ρ shows the existence of local concentrations of electronic charge in both the bonded and nonbonded regions of an atom in a molecule. It has also been found that the number, relative size and locations of the bonded and nonbonded charge concentrations in the valence shell of an atom in a molecule are in more or less general agreement with the localized pair model and with Gillispie's theory of molecular geometry.³

The EFG is determined mainly by the asymmetric distributions of the valence electrons because the closed shells are expected to have spherical symmetry² at least in the light atoms like N. Therefore, it is reasonable to expect a relationship between the Laplacian of ρ about each quadrupolar nucleus and the corresponding EFG at that nuclear site. In this work such a relationship is explored for a set of nitriles with $R = B, H, CN, HCO$, the *Z* form of iminoacetonitrile (IACN), CCH, CH_3, NH_2, FO, OH , and F .

COMPUTATIONAL DETAILS

The charge distributions were obtained from self-consistent field (SCF) calculations that employed the MONSTERGAUSS program⁷ with a 4-31G** basis set with standard exponents and factors.⁸ Experimental values for the bond lengths and bond angles were used when available.⁹ For $R = HO, HCO$, and *Z*-IACN, optimized geometries already reported where used while for $R = FO$, the optimized geometry was that corresponding to a STO-3G basis set.¹⁰

The topological properties of ρ were calculated with a modified version of the EXTREME program and plotted with the PLOTDEN and SCHUSS programs of the AIMPAC package.^{11,12} The components of the EFG produced by the topologically defined atoms were calculated with a modified version of the PROAIM program.^{11,12} All the calculations were made with an IBM 3081RX/VM 370 computer.

THE TOPOLOGY OF THE CHARGE DENSITY

The topological properties of the molecular electronic charge distribution are displayed by its gradient field.^{4,5} Every gradient path originates and terminates at critical points in $\rho(\mathbf{r})$; these points are such that $\nabla\rho(\mathbf{r}) = 0$. A critical point is classified by the eigenvalues (λ_i) of the Hessian

^{a)} On leave from the Departamento de Química, Facultad Experimental de Ciencias, Departamento de Química, Universidad del Zulia, Maracaibo, Venezuela.

^{b)} To whom all correspondence should be addressed.

matrix formed with the second derivatives^{4,5} of $\rho(\mathbf{r})$. In molecules which do not possess ring or cage structures only two types of critical points are found. These points labeled by their rank (number of nonzero eigenvalues) and signature (excess number of positive over negative eigenvalues) are $(3, -1)$ and $(3, -3)$. A $(3, -3)$ point represents a local maximum in $\rho(\mathbf{r})$, while $(3, -1)$ points represent local maxima in two directions and local minima in the third direction and are called bond critical points.^{4,5} The $(3, -3)$ points occur generally at the nuclear positions so that each nucleus is a point attractor in the vector field $\nabla\rho(\mathbf{r})$. Therefore, all the gradient paths in the vicinity of a given nucleus terminate at that nucleus. The region transversed by the gradient paths which terminate at a given attractor is called the basin. A molecule could be therefore uniquely partitioned into basins each of which contains only one attractor point or nucleus. An atom is then defined as the union of an attractor and its associated basin.^{4,5} On the other hand, the set of all the gradient paths which terminates at a bond critical point between atoms A and B determines the interatomic surface S_{AB} while the atomic surface S_A of atom A is defined as the boundary of its basin. The atomic surface that has zero flux in the gradient vectors of $\rho(\mathbf{r})$ provides a suitable definition of atoms in molecules that gives particular quantum mechanical properties to these fragments.^{4,5}

On the other hand, the Laplacian provides information about regions wherein the charge is depleted or concentrated without having to recur to arbitrary reference states.^{3,6} In free atoms, the Laplacian describes the shell structure as pairs of shells of charge concentration and depletion.³ The interaction between atoms may be characterized through a study⁶ of the Laplacian of ρ . The negative curvatures of ρ at the critical point, $(\lambda_1 \text{ and } \lambda_2)$, measure the degree of contraction of the charge density in the interatomic surface, perpendicular to the interaction line towards the critical point. The positive curvature (λ_3) measures the degree of contraction of ρ parallel to the interaction line away from the critical point and towards each of the neighboring nuclei⁶. If λ_1 and λ_2 dominate, ρ is locally concentrated in the region of the critical point and the potential energy in this region has relatively large negative values. In this case, the atomic interaction is dominated by the low potential energy resulting from the formation of the interatomic critical point.⁶ If the positive curvatures dominate, ρ is concentrated separately in each of the atomic basins and the interaction is dominated by the relatively large positive contributions to the kinetic energy of the molecule. A positive $\nabla^2\rho(r_c)$ describes an ionic bond while a negative value describes a covalent bond between the atoms involved.⁶ For interactions with negative $\nabla^2\rho(r_c)$, the values of $|\lambda_1|/\lambda_3$ are larger than 1 while $\rho(r_c)$ is large. In some bonds, the critical point is located close to or at the nodal surface in $\nabla^2\rho$ and the atomic basins neighboring the interatomic surface exhibit opposite behavior with respect to the sign of the Laplacian.⁶ In that case, $\rho(r_c)$ is large although the Laplacian is positive at the critical point while $|\lambda_1|/\lambda_3$ have values intermediate between those found in the other interactions. For that reason, these bonds are called intermediate in the description based in the topology of ρ .

TOPOLOGICAL PROPERTIES OF BONDS IN NITRILES

From Table I it is seen that the properties of ρ at the critical point r_c of the CN bond are only slightly perturbed by substitution. The position of the critical point varies about 0.749 a.u. while the value of the density $\rho(r_c)$ about 0.470 a.u. In terms of the localized pair of electrons model the high values of $\rho(r_c)$ reflects the presence of multiple bonding in the CN fragment.⁶ The values of the ratio $|\lambda_1|/\lambda_3$ correspond, as expected, to those found in covalent bonds but of the intermediate type.⁶

In contrast, the R-C bond properties show much greater variations as seen also in Table I. In particular, the position of the critical point moves towards the C nucleus as the electronegativity of R fragment increases. As depicted in Fig. 1, the critical point in the B-CN bond is very close to the B atom, in the NCCN (Fig. 2) it is located at the C-C bond midpoint and in the F-CN bond (Fig. 3), the point moves closer to the C atom. This trend reflects the property possessed by the more electronegative atoms or fragments for attracting electrons toward its basins.^{1,13} As in the C-N bond, the relative change in charge densities $\rho(r_c)$ in the R-C bonds produced by the different substituents is slightly less than the relative changes of the position of the critical point.

TABLE I. Topological properties of the charge distribution of bonds in nitriles.^a

R	C-N			R-C		
	r_c	$\rho(r_c)$	$ \lambda_1 /\lambda_3$	r_c	$\rho(r_c)$	$ \lambda_1 /\lambda_3$
B	0.733	0.497	0.368	2.065	0.164	0.476
H	0.745	0.475	0.369	1.315	0.304	2.224
CN	0.749	0.468	0.372	1.314	0.312	2.778
CCH	0.749	0.473	0.383	1.361	0.318	3.028
CH ₃	0.748	0.475	0.389	1.582	0.276	2.740
F	0.752	0.458	0.328	0.777	0.313	0.333
IACN	0.747	0.475	0.383	1.566	0.272	2.409
HCO	0.750	0.468	0.386	1.530	0.283	2.620
NH ₂	0.753	0.468	0.401	0.882	0.342	1.975
HO	0.750	0.463	0.540	0.842	0.306	0.738
FO	0.748	0.459	0.337	0.847	0.293	0.715

R	Bonded		Nonbonded	
	$-\nabla^2\rho$	r_b	$-\nabla^2\rho$	r_{nb}
B	3.127	0.791	3.548	0.739
H	2.612	0.800	3.358	0.743
CN	2.546	0.801	3.436	0.741
CCH	2.533	0.802	3.321	0.744
CH ₃	2.525	0.802	3.239	0.746
F	1.917	0.819	3.057	0.748
IACN	2.600	0.801	3.341	0.743
HCO	2.592	0.800	3.397	0.742
NH ₂	2.230	0.811	3.083	0.748
HO	2.088	0.815	3.082	0.748
FO	2.132	0.812	3.196	0.746

^a The values of the Laplacian of the charge density refer to the bonded (b) and nonbonded (nb) concentration of the N atom. The origin of coordinates is at the C nucleus for quantities related to the critical point while for the Laplacian the origin is at the N nucleus. All quantities are expressed in a.u.

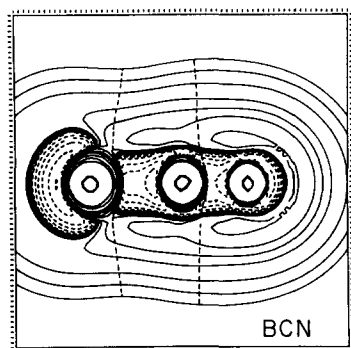


FIG. 1. Contour map of the Laplacian of the charge density for BCN in a plane that contains all the nuclei. Positive values of are denoted by the solid contours, negative values by dashed contours. The contour values in a.u. are ± 0.002 , ± 0.004 , ± 0.008 increasing in powers of 10 to ± 8.000 . The outermost contour is $+0.002$ a.u. The intersection of the interatomic surface of zero flux in $\nabla\rho$ with the plane of the figure (heavy dashed lines) is also shown.

The values of $|\lambda_1|/\lambda_3$ given in Table I, on the other hand, indicate that for $R = B$, FO , OH , and F , the $R-C$ bond is of the intermediate type while in the remaining substituents the bond is covalent.⁶

The above results show that the total electronic charge density around the N atom is only slightly perturbed by the substituents while that of the C atom is noticeably changed. Nevertheless, the total changes in the charge distribution upon substitution produce noticeable variations in the EFG observed at the N nucleus.²

ELECTRIC FIELD GRADIENT

The EFG is a traceless, symmetric second rank tensor whose principal axes are generally chosen such that the components² satisfies the inequalities $|q_{zz}| \geq |q_{yy}| \geq |q_{xx}|$. The five independent components of the EFG consist of the two diagonal terms and three direction cosines linking the principal axes system with an arbitrary frame of reference.² Usually, the coupling constant, $e^2 Q q_{zz}/h$, (where Q is the nuclear electric quadrupole moment), and the asymmetry parameter, $\eta = |(q_{yy} - q_{xx})/q_{zz}|$, are determined experimentally. The coupling constant provides a measure of the intensity of the quadrupole interaction while η reflects the deviation of the EFG tensor from the axial symmetry.²

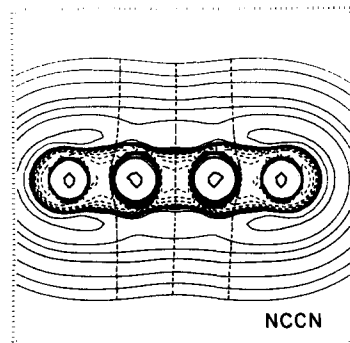


FIG. 2. Contour map of the Laplacian of the charge density for NCCN in a plane that contains all the nuclei. The parameters and other characteristics are equal to those of Fig. 1.

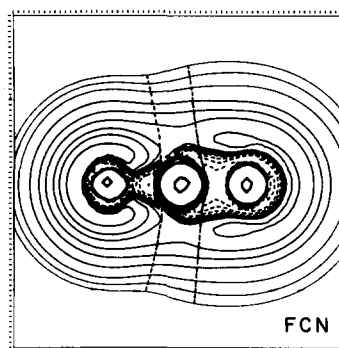


FIG. 3. Contour map of the Laplacian of the charge density for FCN in a plane that contains all the nuclei. The parameters and other characteristics are equal to those of Fig. 1.

It was found that for $R = FO$, the principal z axis of the EFG tensor made an angle of 2° with the $C-N$ direction while for $R = OH$, HCO , and $IACN$ the deviation was between 0.44° and 0.12° . In all the other nitriles studied, the z axis was directed along the $C-N$ bond. The small deviations of the z axis found for $R = FO$, HO , HCO , and $IACN$ produced only a negligible contribution to the diagonal elements when the EFG tensor was rotated so that z axis pointed in the $C-N$ direction. Therefore, all the EFG tensors were assumed to have the principal z axis lying along that direction.

The EFG at any nucleus in an isolated molecule is the result of the electronic contribution of the same atom plus a nuclear and an electronic contribution of each of the atoms present in the molecule. The EFG tensor may be divided into atomic contributions if an adequate partitioning scheme is adopted. In this work, the atoms defined by the zero flux surfaces³⁻⁶ were used to calculate the total EFG at the N nucleus. Examples of intersection of these surfaces with molecular planes for several nitriles are shown in Figs. 1-3. In Table II there are shown the different contributions to the q_{zz} component at the N atom in the nitriles studied in this work. The contribution to the EFG of the N atom coming from atoms beyond the CN group (R) is very small when compared with that produced by the neighboring C atom or by the electrons belonging to the N atom. Nevertheless, the variation in the contribution of R to the N q_{zz} component is similar to that found in the C atom contribution. On the other hand, the variations found in the electronic contribution of the N atom itself is an order of magnitude larger or more than those obtained from the other two contributions as seen in Table II. That difference in magnitude may be explained by considering the type of charges involved in each contribution to the total EFG. The electronic part of the EFG in the N atom is not compensated by any nuclear charge so even a small variation in the symmetry of the N electronic distribution will produce a noticeable variation in the EFG components. This effect in the N atom is further reinforced by the r^{-3} factor present in the EFG operator that enhances heavily any change occurring close to the quadrupolar nucleus.² The total contribution of the other atoms to the N EFG is just the difference between their individual electronic and nuclear contributions. For that reason, in neutral molecules, the total contribution coming from the other atoms is quite small as seen in Table II. On the other hand, this contribution is also further diminished by the r^{-3}

TABLE II. Calculated values of the different contributions to q_{zz} at the N atom in the CN group.^a

R	$(eq_{zz})_R$	$(eq_{zz})_C$	$(eq_{zz})_N$	$(eq_{zz})_T$
B	0.026 ^b	0.539 ^b	- 1.790	- 1.225
	- 0.047 ^c	- 0.671 ^c		
	0.073 ^d	1.210 ^d		
H	0.008	0.524	- 1.533	- 1.001
	- 0.018	- 0.630		
	0.026	1.130		
CN	0.011	0.503	- 1.531	- 1.017
	- 0.136	- 0.627		
	0.147	1.142		
CCH	0.011	0.519	- 1.472	- 0.942
	- 0.098	- 0.623		
	0.109	1.142		
CH ₃	0.013	0.513	- 1.435	- 0.908
	- 0.110	- 0.635		
	0.123	1.148		
F	- 0.022	0.541	- 1.113	- 0.594
	- 0.210	- 0.601		
	0.188	1.142		
IACN	0.015	0.512	- 1.510	- 0.983
	- 0.136	- 0.636		
	0.151	1.148		
HCO	0.015	0.499	- 1.534	- 1.020
	- 0.141	- 0.629		
	0.156	1.127		
NH ₂	- 0.016	0.535	- 1.239	- 0.720
	- 0.166	- 0.604		
	0.150	1.140		
HO	- 0.018	0.541	- 1.187	- 0.664
	- 0.178	- 0.601		
	0.160	1.142		
FO	- 0.016	0.534	- 1.258	- 0.740
	- 0.222	- 0.604		
	0.206	1.139		

^a $(q_{zz})_R$ corresponds to the contribution of the rest of the molecule to the q_{zz} component, $(q_{zz})_C$ to that of the neighboring C atom while $(q_{zz})_N$ is the electronic contribution of the N atom. All quantities are expressed in a.u.

^bTotal contribution.

^cElectronic contribution.

^dNuclear contribution of each atom or fragment.

factor of the EFG operator so that only neighboring atoms may produce a noticeable effect. In nitriles, the total contribution due to the neighboring C atom is of about 30% to 40% of that corresponding to the N electronic contribution to the EFG. Nevertheless, even if the C atom showed upon

substitution noticeable changes in its charge distribution, (see Figs. 1–3), those changes did not produce noticeable variations in the N EFG. Those changes are not significant because they are strongly reduced by the combined effect of the r^{-3} factor and the cancellation produced by the nuclear charge of the C atom. Therefore the EFG present at the N nucleus reflects primarily the changes in the N electronic distribution (or equivalently, in the shape and content of the basin) produced by the substituents either through charge transfer or/and polarization.

The q_{yy} and q_{xx} components of the EFG at the N nucleus obtained in several nitriles are shown in Table III. As in q_{zz} the neighboring C atom produced a noticeable contribution to the q_{yy} and q_{xx} component but of different sign than that corresponding to the electronic contribution of N. In FOCN, HOCN, and NH₂CN, the N contribution to the q_{xx} is close in absolute value to that produced by the neighboring C atom. Therefore, the total value of q_{xx} is low and a high value for the asymmetry parameter η is found in those nitriles. Consequently, the changes in the N electronic contribution rather than the changes in the neighboring C atom or in the rest of the molecules are the main cause of the lack of axial symmetry of the N EFG tensor.

Measured or calculated EFGs have been usually interpreted in terms of models which generally involve either bonded or nonbonded² localized electron pairs. Nevertheless, an interpretation of the EFG directly in terms of the total charge density has not been undertaken. This is understandable because the total density gives no indication of the concentration of charge predicted by the Lewis electron pair model.^{3–6} Nevertheless, the Laplacian amplifies any local variation in the density, thus, unveiling even minute changes.^{3,6} Therefore, the study of $\nabla^2\rho$ provides the adequate framework within which the EFG changes may be interpreted in terms of the total charge distribution.

The Laplacian^{3,6} of ρ shows that in an isolated atom there exists a number of alternating pairs of shells of charge depletion and concentration. The valence shell of an isolated atom is a sphere on whose surface the charge concentration is maximal. If that distribution is spherically symmetric, no EFG is generated at the nucleus of the atom. The formation of bonds alters the atomic valence shells and a number of local maxima and minima are present on the corresponding surface of maxima charge concentration.^{3,6} The number of the maxima of $\nabla^2\rho$, relative position and size yields a replica of the Lewis model of bonded and nonbonded electron pairs.^{3,6} Nevertheless, although the Laplacian of ρ mimics, in many respects, the spatial properties of equivalent or localized molecular orbitals, the two descriptions are not to be equated directly.³

In nitriles, only two maxima in $-\nabla^2\rho$ (maxima in charge density) are present within the N basin and near the N nucleus in the C–N direction (z axis). A bonded maximum is located towards the C atom and a nonbonded one resembling a “lone pair” is located in the opposite direction; this is seen in Figs. 4–6. Other bonded and nonbonded maxima are also located in the remaining atoms of the molecule as seen in the same figures. In Table I the position and the values of the bonded and nonbonded maxima found next to

TABLE III. Calculated values of the different contributions to q_{xx} and q_{yy} at the N atom in the CN group.^a

R	$(eq_{xx})_R$	$(eq_{xx})_C$	$(eq_{xx})_N$	$(eq_{xx})_T$	$(eq_{yy})_R$	$(eq_{yy})_C$	$(eq_{yy})_N$	$(eq_{yy})_T$
B	-0.015	-0.267	0.895	0.613	-0.015	-0.267	0.895	0.613
H	-0.004	-0.242	0.767	0.501	-0.004	-0.242	0.767	0.501
CN	-0.006	-0.252	0.767	0.509	-0.006	-0.252	0.767	0.509
CCH	-0.010	-0.255	0.736	0.471	-0.010	-0.255	0.736	0.471
CH ₃	-0.008	-0.256	0.718	0.454	-0.008	-0.256	0.718	0.454
F	0.010	-0.270	0.557	0.297	0.010	-0.270	0.557	0.297
IACN	-0.005	-0.255	0.716	0.456	-0.010	-0.257	0.794	0.794
HCO	-0.009	-0.248	0.620	0.363	-0.005	-0.251	0.914	0.658
NH ₂	0.009	-0.266	0.285	0.028	0.007	-0.270	0.935	0.692
HO	0.006	-0.265	0.448	0.185	0.011	-0.271	0.739	0.471
FO	0.008	-0.266	0.369	0.111	0.009	-0.269	0.889	0.700

^a $(q_{ii})_R$, ($i = x, y$), corresponds to the contribution of the rest of the molecule to the q_{ii} component, $(q_{ii})_C$ to that of the neighboring C atom while $(q_{ii})_N$ is the electronic contribution of the N atom. All quantities are expressed in a.u.

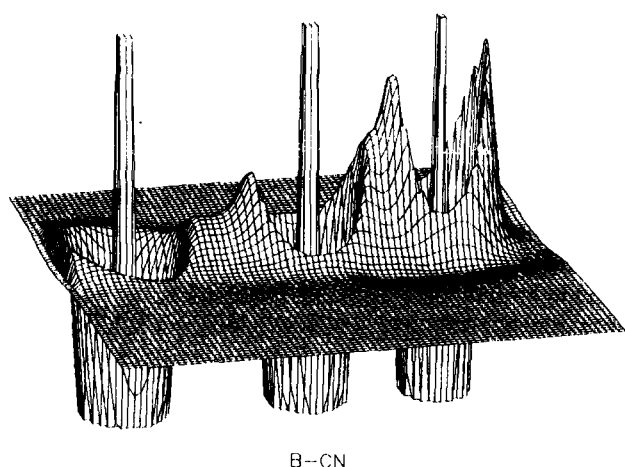


FIG. 4. Relief map of $-\nabla^2\rho$ in the same plane of Fig. 1 for BCN. A bonded maximum is observed in the region between the N and the C atoms that belongs to the N valence shell. Also a nonbonded maximum in the N valence shell equivalent to the lone pair in the theory of Lewis may be seen in the figure.

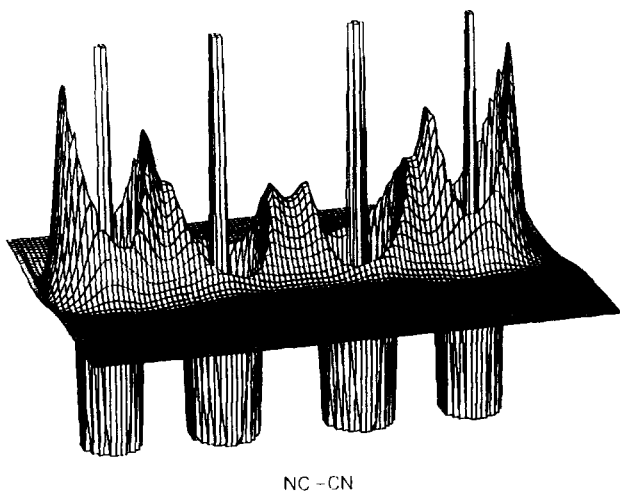


FIG. 5. Relief map of $-\nabla^2\rho$ in the same plane of Fig. 2 for NCCN. A noticeable change in the bonded maximum of the N valence shell is seen when compared with the map of BCN.

the N atom and along the z axis are also shown. From Figs. 4–6, we see that the different substituents modify the size of *both* maxima and in a much lesser degree also their positions. The values of the EFG at the N atom reflect the asymmetry of the charge distributions present around the nucleus. It is expected then that a correlation will be found between the position and size of the maxima of $-\nabla^2\rho$ corresponding to the valence shell along the z axis and the q_{zz} component of the EFG. The fact that the position of the maxima showed only negligible changes with substitution indicated that this contribution to the changes in q_{zz} may be taken as constant in nitriles. Therefore, only the sizes of the maxima were considered in the correlation. Figure 7 shows that an excellent correlation exists ($r = 0.999$) between the sum of the values of the bonded and nonbonded maxima of $-\nabla^2\rho$ and the changes in the q_{zz} component at the N nucleus when HCN is taken as a reference. This shows that the q_{zz} component at the N atom in nitriles is determined by the values of both the bonded and nonbonded maxima in charge density located in the z axis. It is interesting to notice that the maxima taken

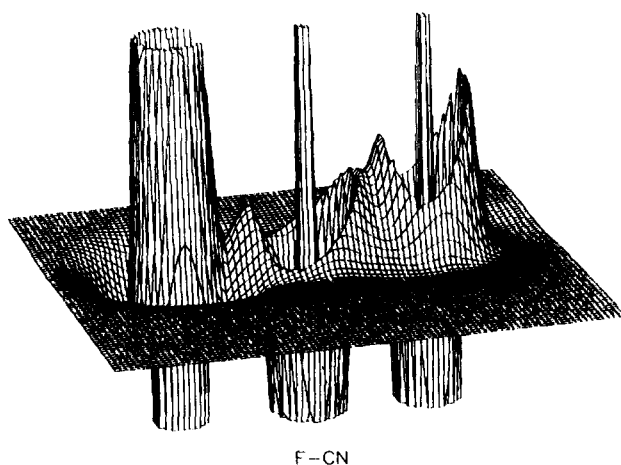


FIG. 6. Relief map of $-\nabla^2\rho$ in the same plane of Fig. 3 for FCN. A noticeable change in both maxima of the N valence shell is seen when compared with the map of BCN.

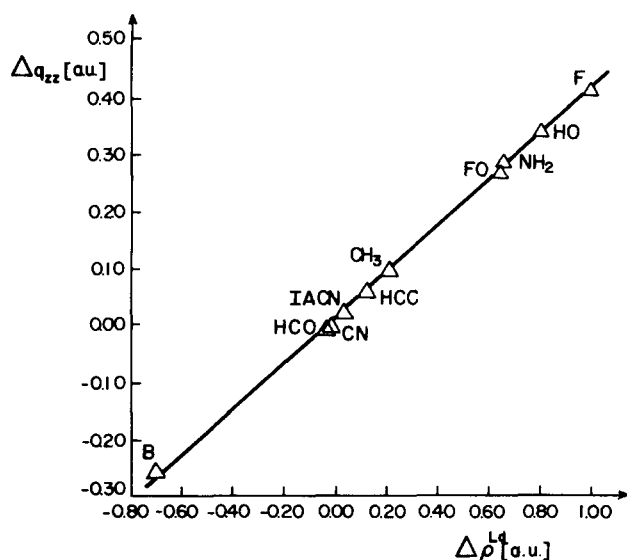


FIG. 7. Plot of $\Delta q_{zz} = (q_{zz} - q_{zz}^0)$ vs $\Delta \rho^{Ld} = (\nabla^2 \rho_b + \nabla^2 \rho_{nb})$. The straight line corresponds to $\Delta q_{zz} = 0.406 \Delta \rho^{Ld} + 0.016$ with $r = 0.999$. q_{zz}^0 corresponds to value obtained in HCN.

separately do not correlate well with the changes in q_{zz} . This is a direct consequence of the fact that both maxima were found to be affected by substitution in different ways as seen in Table I. This result clearly casts doubts about the usual assumption made in the Townes and Dailey theory² that the N lone pair does not change its population and shape upon substitution.

In linear nitriles, all the regions of charge depletion and concentration that contribute to the other two components are symmetric around the z axis so that $q_{xx} = q_{yy}$ as seen in

TABLE IV. Values and positions of the maxima in the charge density of the N valence shell on the x and y axes perpendicular to the C–N direction and containing the N nucleus.

R	$-\nabla^2 \rho_{\max}$	x	$-\nabla^2 \rho_{\max}$	x
B	0.7156	−0.8181	0.7156	0.8181
H	0.8084	−0.8142	0.8084	0.8142
CN	0.8119	−0.8141	0.8119	0.8141
CCH	0.8333	−0.8132	0.8333	0.8132
CH ₃	0.8442	−0.8124	0.8453	0.8124
F	0.9781	−0.8069	0.9781	0.8069
IACN	0.8469	−0.8123	0.8489	0.8123
HCO	0.9285	−0.8091	0.9304	0.8086
NH ₂	1.2021	−0.7980	1.2178	0.7973
HO	1.0697	−0.8030	1.0697	0.8030
FO	1.1443	−0.8001	1.1443	0.8030

R	$-\nabla^2 \rho_{\max}$	y	$-\nabla^2 \rho_{\max}$	y
B	0.7156	−0.8181	0.7156	0.8181
H	0.8084	−0.8142	0.8084	0.8142
CN	0.8119	−0.8141	0.8119	0.8141
CCH	0.8333	−0.8132	0.8333	0.8132
CH ₃	0.8448	−0.8124	0.8448	0.8124
F	0.9781	−0.8069	0.9781	0.8069
IACN	0.7891	−0.8151	0.7891	0.8151
HCO	0.6956	−0.8200	0.6956	0.8200
NH ₂	0.6524	−0.8219	0.6524	0.8219
HO	0.8215	−0.8136	0.8303	0.8133
FO	0.7051	−0.8196	0.7083	0.8189

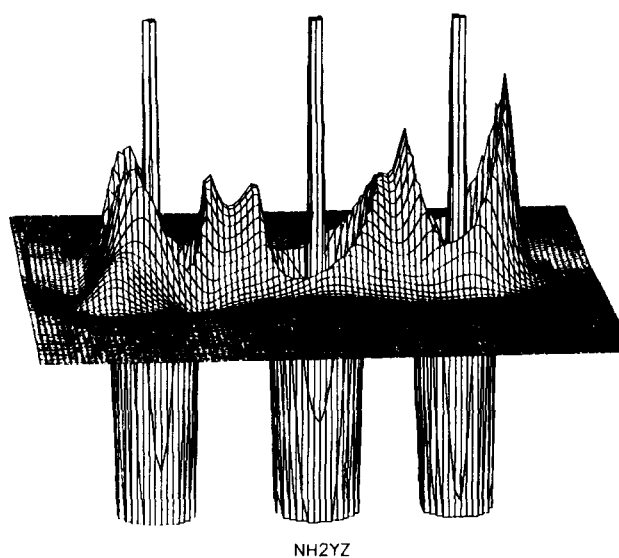


FIG. 8. Relief map of $-\nabla^2 \rho$ in a plane that contains the N, C, and N nuclei in NH_2CN and is parallel to the H–H direction (plane yz).

Table IV. In the nonlinear nitriles, some of these maxima and minima are of different sizes as shown in Table IV and lack symmetry around the z axis; this is indicated also in Figs. 8 and 9. The bonded and nonbonded regions of charge concentration encountered along the z axis have cylindrical symmetry around that axis and hence its contribution to both q_{xx} and q_{yy} is similar. The asymmetry in the EFG components therefore arises from the differences present in the N valence shell in those regions which are perpendicular to the z axis. This asymmetry is particularly noticeable in NH_2CN where a large value of η (0.92) was found as a result of the asymmetry in the charge distribution produced by the interaction between the NH_2 and the CN groups. From Figs. 8

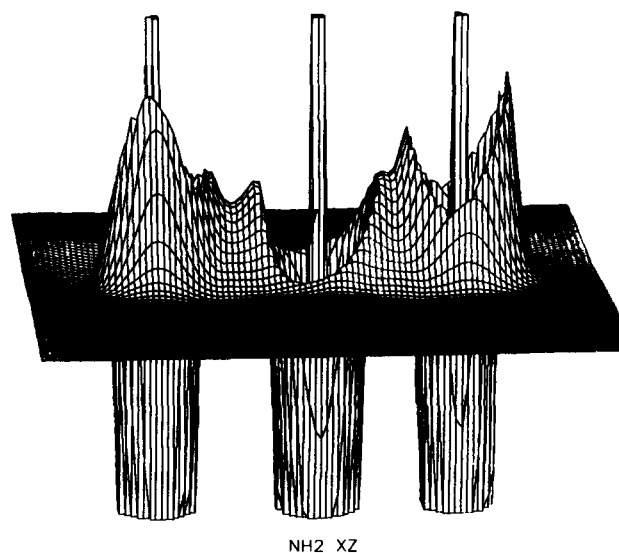


FIG. 9. Relief map of $-\nabla^2 \rho$ in a plane that contains the N, C, and N nuclei in NH_2CN and is perpendicular to the H–H direction (plane xz). The N valence shell is noticeably higher in a direction perpendicular to the C–N bond than in the yz plane shown in Fig. 8.

and 9 we see that the valence shell of the N atom of the nitrile group is quite different in planes perpendicular to the z axis that contain the N nucleus. Therefore, the value of q_{xx} and q_{yy} differed markedly and a high value for η was found for this nitrile. A similar effect involving the N valence shell concentration was found for all the other nonlinear nitriles that have finite values of η . From Figs. 8 and 9 may be seen that two maxima in the Laplacian of the valence shell charge are present in the xz and in the yz planes containing the N nucleus. In the first step of the correlation procedure, the maxima in each plane were added. In the second step, the difference between these values found for each plane were plotted against the corresponding $|q_{xx} - q_{yy}|$ values. An excellent correlation ($r = 1.000$) was found between these values for the nitriles studied in this work. A similar correlation ($r = 0.992$) was also found between the same difference in the maxima of $-\nabla^2\rho$ and η . Therefore, the asymmetry parameter of the N EFG tensor in nitriles is determined by the asymmetry of the valence shell in planes perpendicular to the z axis.

All the above results showed that there is a direct relationship between the charge topology reflected in its Laplacian and the components of the EFG at the N nucleus in nitriles. Clearly, this shows that the EFG tensors can be interpreted directly in terms of an observable like ρ . The present interpretation is model independent and therefore free from the shortcomings present in models based in quantities which are not observables like orbitals and their population.²

ACKNOWLEDGMENTS

We thank the Centro Científico de IBM de Venezuela for a generous grant of computer time, Professor R. F. W.

Bader, MacMaster University, Hamilton, Canada, for a copy of the AIMPAC package of programs, and to E. Ludeña for useful comments.

¹R. L. DeKock and H. B. Gray, *Chemical Structure and Bonding* (Benjamin, New York, 1980).

²E. A. C. Lucken, *Nuclear Quadrupole Coupling Constant* (Academic, New York, 1969).

³R. F. W. Bader, P. J. MacDougall, and C. D. H. Lau, *J. Am. Chem. Soc.* **106**, 1594 (1984).

⁴R. F. W. Bader, T. T. Nguyen-Dang, and Y. Tal, *Rep. Prog. Phys.* **44**, 895 (1981).

⁵R. F. W. Bader, *Acc. Chem. Res.* **18**, 9 (1985).

⁶R. F. W. Bader and H. Essen, *J. Chem. Phys.* **80**, 1943 (1984).

⁷MONSTERGAUSS 82, M. Petersen and R. Poirier, Department of Chemistry, University of Toronto, Toronto, Ontario, Canada, 1982.

⁸R. Ditchfield, W. J. Hehre, and J. A. Pople, *Chem. Phys.* **54**, 724 (1970).

⁹For HCN, CH₃CN, the data was obtained from C. C. Costain and B. P. Stoichef, *J. Chem. Phys.* **30**, 777 (1959); for FCN, HCCCN, from J. K. Tyler and J. Sheridan, *Trans. Faraday Soc.* **59**, 2661 (1959); NH₂CN, J. K. Tyler, J. Sheridan, and C. C. Costain, *J. Mol. Spectrosc.* **43**, 248 (1972); while for NCCN from Y. Morino, K. Kuchitsu, Y. Hori, and M. Tamimoto, *Bull. Chem. Soc. Jpn.* **41**, 2349 (1968).

¹⁰For HOCN, FOCN, data obtained from D. Poppinger and L. Radom, *J. Am. Chem. Soc.* **101**, 3674 (1978); for HCOCN, from M. Eiseinstein and F. L. Hirshfeld, *J. Comput. Chem.* **4**, 15 (1983); while for Z-IACN, from J. B. Moffat, *J. Chem. Soc. Chem. Comm.* **21**, 888 (1975).

¹¹F. W. Biegler-König, R. F. W. Bader and T. H. Tang, *J. Comput. Chem.* **3**, 317 (1982).

¹²R. F. W. Bader, T. H. Tang, Y. Tal, and F. W. Biegler-König, *J. Am. Chem. Soc.* **104**, 946 (1982).

¹³R. S. Boyd and K. E. Edgecombe, *J. Am. Chem. Soc.* **110**, 4182 (1988).